26 May 2010, 4:45 pm - 6:45 pm

Multi-Modal Synthesis and Variable Modulus Effects in Resonant Column Tests by Random Excitations

Jeramy C. Ashlock
Iowa State University, Ames, IA

Ronald Y. S. Pak
University of Colorado at Boulder, Boulder, CO

Fifth International Conference on
Recent Advances in Geotechnical Earthquake Engineering and Soil Dynamics
and Symposium in Honor of Professor I.M. Idriss
May 24-29, 2010 • San Diego, California

MULTI-MODAL SYNTHESIS AND VARIABLE MODULUS EFFECTS IN RESONANT COLUMN TESTS BY RANDOM EXCITATIONS

Jeramy C. Ashlock
Iowa State University
Ames, IA 50011

Ronald Y. S. Pak
University of Colorado at Boulder
Boulder, CO 80309

ABSTRACT

To extend current measurement and data synthesis techniques for resonant column testing, random vibration transfer functions measured using a modified 6 inch (152.4 mm) diameter Drnevich free-free resonant column device are evaluated against viscoelastic theories of homogeneous and heterogeneous soil models. By means of the transfer function approach, it is found that the first four resonant peaks of the soil column response can be captured experimentally with some instrumental adaptations. By calibration against theoretical transfer functions, the ability to characterize the modulus and damping properties of the soil samples over a broad range of frequencies is demonstrated. As a generalization of the analytical theory for resonant column tests to a number of practical applications, the sensitivity of the experimental procedure to the specimen's vertical material heterogeneity is examined for a linear variation in shear modulus. The feasibility of applying the experimental and analytical techniques to investigations of the frequency-dependence of damping properties is demonstrated. Calibration of theoretical models against measured resonant column soil behavior over a wide range of frequencies is anticipated to lead to more accurate material characterization across the spectrum of frequencies encountered in seismic and foundation vibration applications.

INTRODUCTION

In problems of soil dynamics and earthquake engineering, characterization of the soil's modulus and damping properties are often of critical importance. Various forms of resonant column (RC) test methods have been widely studied and commonly used to obtain measurements of modulus and damping as functions of controlling parameters such as confining pressure and shear strain, among others (Hardin 1965, Drnevich et al. 1978, ASTM D 4015). While resonant column and other dynamic laboratory tests commonly involve sinusoidal loading, natural and man-made sources such as earthquakes, wind, waves, and traffic often give rise to non-periodic loadings covering a wide range of excitation frequencies. It is therefore of interest to ascertain whether the use of random and impulse excitation types in laboratory tests can provide measured dynamic soil properties that more accurately reflect those that will control the response in the field. While random excitations along with output-only or input-output transfer function techniques have been applied to resonant column tests in the past (e.g. Yong et al. 1977, Al-Sanad et al. 1983, Aggour et al. 1988, 1989, Amini et al. 1988, Cascante and Santamarina 1997, Li et al, 1998, Rix and Meng 2003, Wang et al. 2003, Cascante et al. 2005) they have typically involved the use of fixed-free apparati and were usually focused on measurements of the fundamental resonant peak. Because the bottom end of the sample is restrained from rotation in fixed-free RC devices, corresponding transfer function techniques generally involve the measurement of both the input and output quantities at the top of the sample. These quantities are typically in the form of the top-platen's rotational motion and the applied torque, obtained by applying a torque-current calibration factor to a voltage measured within the electromagnet drive circuit. If the drive-circuit voltage with respect to ground is used instead of the voltage drop across a power resistor, one must also contend with distortions of the measured damping ratios caused by the effects of back-emf (e.g., Cascante et al. 1997, 2003, Wang et al. 2003). Correction for back-emf effects requires additional device-dependent calibrations of the coil inductance and resistance, which are usually approximated as frequency independent. It should be noted that a measurement of the input current as specified in ASTM D 4015 will implicitly account for the back-emf effect. Therefore, the back-emf transfer function corrections are only required if input voltage is measured instead of current (Li et al. 1998, Cascante et al. 2005). For the common fixed-free type of RC device, other issues such as effects of eddy currents (Cascante et al. 2005) and radiation of energy through the base due to a lack of perfect fixity can also affect measurements of damping

(Drnevich 1978, Cascante et al. 2003, Wang et al. 2003, Khan et al. 2008).

EXPERIMENTAL METHODS

The need for device-dependent torque-current calibration factors as well as the problems of back-emf and base fixity can be avoided by a direct measurement of the physical transfer function of the soil column. The free-free or Drnevich type of resonant column device can be adapted to provide a direct transfer function measurement, as it features transmission of motion from the bottom platen to the top platen through the soil sample by design. This can be achieved with minor modifications to accommodate measurement of the rotational motion of the platens using transducers of sufficient sensitivity. In this study, a 6-inch diameter free-free Drnevich type RC device was modified by attaching four instrumentation blocks with stud-mounted PCB model 352C67 accelerometers to opposite sides of the top and bottom platens. The traditional RC system's signal generator, frequency counter, and oscilloscope were replaced with two Spectral Dynamics SigLab spectrum analyzers with 20 kHz bandwidth random excitation and measurement capabilities. A random voltage signal of selected rms amplitude was generated by the SigLab unit, then amplified by a Techron 5515 power amplifier and sent to the drive coils of the resonant column device. The resulting time-histories of the tangential accelerations from the bottom (active) and top (passive) platens were digitized and recorded using a 2 kHz analysis bandwidth with 4096 samples in the time-domain, a sampling rate of 5.12 kHz, and a frequency resolution of 1.25 Hz. Analog low-pass filters and Hanning windowing were used to minimize the effects of aliasing and spectral leakage. Experimental noise was further minimized by using 30 ensemble averages of spectral quantities in each test. From the digitized signals, the auto-spectral densities $G_{xx}(f)$ and $G_{yy}(f)$ and cross-spectral densities $G_{yx}(f)$ were calculated, in which $x(t)$ and $y(t)$ denote stimulus and response signals and f is the frequency in Hz. The transfer functions (also referred to as frequency-response functions or FRF),

$$H_{yx}(f) = \frac{\bar{G}_{yx}(f)}{\bar{G}_{xx}(f)} \tag{1}$$

were calculated along with coherence functions, defined by

$$\gamma^2_{yx}(f) = \frac{|\bar{G}_{yx}(f)|^2}{\bar{G}_{xx}(f)\bar{G}_{yy}(f)}\ , \tag{2}$$

in which bars denote spectral averages (Bendat and Piersol, 1986). The symmetric arrangement of the four accelerometers allowed spurious transfer function peaks caused by lateral bending modes of the sample to be averaged out. To minimize the influence of particle-size effects, a large sample of dry silica sand (G_s = 2.65) was used, having a radius r =76.6 mm, height h =315.1 mm, density ρ = 1707 kg/m^3, void ratio e = 0.55 and relative density D_R = 79.6%. Effects of large shear strains were minimized by testing under small-strain random vibration at confining pressures of 10, 15, 20, 30, 40 and 50 psi (68.9, 103.4, 137.9, 206.8, 275.8 and 344.7 kPa). More details about the tests can be found in Ashlock and Pak (2010).

With the above described test procedure and modifications to the RC device, the transfer functions of the soil column can be measured directly and evaluated against analytical transfer functions without requiring the consideration of electro-mechanical interaction, torque-current calibration factors or the effects of base radiation or back-emf.

THEORETICAL TRANSFER FUNCTIONS FOR LINEAR SHEAR MODULUS PROFILE

Although various resonant column sample preparation techniques are used in an effort to achieve homogeneity, it is difficult to completely avoid some variations in density and confining stress throughout the sample volume. Additionally, the increase in mean principal stress with depth due to the soil's self-weight will cause a depth-wise increase in shear modulus (e.g. Hardin and Richart, 1963, Hardin and Drnevich 1972). While the effects of such heterogeneities may be negligible for typical small-scale resonant column samples on the order of a few inches in height, they may be of interest for larger samples on the order of 1 ft (30 mm) in height in combination with low confining pressures. To investigate the effects of a vertical heterogeneity in shear modulus on the transfer functions of the soil sample, a linear variation in shear modulus of the form

$$G(z) = G_0\left(1 + m\frac{z}{h}\right), \qquad m \geq -1 \tag{3}$$

is considered analytically, with h being the height of the soil sample. In Equation (3), the axial coordinate z is directed upward with the origin at the bottom of the soil sample, and m is a dimensionless heterogeneity parameter. For torsion of a viscoelastic soil sample having a Kelvin-Voigt viscous damping coefficient η, the shear stress $\tau_{z\theta}$ may be expressed as

$$\tau_{z\theta}(r,z,t) = G(z)\gamma(r,z,t) + \eta\dot{\gamma}(r,z,t) \tag{4}$$

where $\gamma(r,z,t) = r\partial\theta_R(z,t)/\partial z = r\partial\theta(z,t)/\partial z$ is the shear strain, $\theta_R(z,t)$ is the angular displacement relative to the base, and $\theta(z,t)$ is the absolute angular displacement relative to a fixed reference frame. The equation of motion in terms of the total angular displacement may then be formulated as

$$\frac{\partial}{\partial z}\left(G(z)\frac{\partial\theta}{\partial z}\right) + \eta\frac{\partial^3\theta}{\partial t\partial z^2} = \rho\frac{\partial^2\theta}{\partial t^2}, \tag{5}$$

in which ρ is the mass density of the soil. Assuming a time-harmonic steady-state solution of the form $\theta(z,t) = \tilde{\theta}(z)e^{i\omega t}$ where $\omega = 2\pi f$ is the circular frequency and $i = \sqrt{-1}$, Equations (3) and (5) give

$$\left(1 + m\frac{z}{h} + i\frac{\omega\eta}{G_0}\right)\frac{d^2\tilde{\theta}}{dz^2} + \left(\frac{m}{h}\right)\frac{d\tilde{\theta}}{dz} + \frac{\omega^2}{C_{s0}^2}\tilde{\theta} = 0 \tag{6}$$

in the frequency domain, where $C_{s0}^2 = G_0 / \rho$ is a reference shear wave speed. For a more general treatment of damping, the term $\omega\eta / G_0$ in Equation (6) may be replaced with the general frequency-dependent form $2\xi(\omega)$, where $\xi(\omega)$ is a generalized damping ratio. One may take $\xi(\omega) = \omega\eta / (2G_0)$ for constant viscous Kelvin-Voigt type damping, or use a constant $\xi(\omega) = \xi_0$ for hysteretic damping behavior. Imposing the inertial boundary condition for the top platen having a polar mass moment of inertia I_t results in

$$\left.\frac{d\tilde{\theta}(z)}{dz}\right|_{z=h} = \frac{\bar{I}\bar{\omega}^2}{h\left(1 + m\frac{z}{h} + i\,2\xi(\omega)\right)}\tilde{\theta}(h), \tag{7}$$

where $\bar{I} = I_t / (\rho h J)$ is the platen-to-soil inertia ratio, J is the polar second moment of area of the sample, and

$$\bar{\omega} = \frac{\omega h}{C_{s0}} \tag{8}$$

is a dimensionless frequency parameter. To facilitate calibration of C_{s0} via comparison with measured transfer functions, it is more convenient to express Equation (6) as

$$\left(1 + m\frac{z}{h} + i2\xi(\bar{\omega})\right)\frac{d^2\tilde{\theta}}{dz^2} + \left(\frac{m}{h}\right)\frac{d\tilde{\theta}}{dz} + \frac{\bar{\omega}^2}{h^2}\tilde{\theta} = 0. \tag{9}$$

The general solution to the above equation is

$$\tilde{\theta}(z) = C_1 I_0\left(i\frac{2\bar{\omega}}{|m|}\sqrt{\mu(z,\bar{\omega})}\right) + C_2 K_0\left(i\frac{2\bar{\omega}}{|m|}\sqrt{\mu(z,\bar{\omega})}\right), \tag{10}$$

where C_1 and C_2 are arbitrary constants, I_n and K_n are the modified Bessel functions of order n of the 1st and 2nd kinds, respectively, and

$$\mu(z,\bar{\omega}) = 1 + \frac{mz}{h} + i2\xi(\bar{\omega}). \tag{11}$$

Prescribing the top boundary condition of Equation (7) along with the base excitation as

$$\theta(0,t) = \tilde{\theta}(0)e^{i\omega t} = \tilde{\theta}_b e^{i\omega t}, \tag{12}$$

while expressing the rotation at the top of the sample as

$$\theta(h,t) = \tilde{\theta}(h)e^{i\omega t} = \tilde{\theta}_t e^{i\omega t}, \tag{13}$$

the transfer function of rotational displacement (or equivalently, tangential acceleration) may be obtained as

$$\frac{\theta(h,t)}{\theta(0,t)} = \frac{\tilde{\theta}_t}{\tilde{\theta}_b} = \frac{2\mu_t\left(I_1(\bar{\omega}_t)K_0(\bar{\omega}_t) + I_0(\bar{\omega}_t)K_1(\bar{\omega}_t)\right)}{\left(\begin{array}{l}2\mu_t\left(I_1(\bar{\omega}_t)K_0(\bar{\omega}_b) + I_0(\bar{\omega}_b)K_1(\bar{\omega}_t)\right) \\ + m\bar{I}\,\bar{\omega}_t\left(I_0(\bar{\omega}_t)K_0(\bar{\omega}_b) - I_0(\bar{\omega}_b)K_0(\bar{\omega}_t)\right)\end{array}\right)}, \tag{14}$$

where I_n and K_n are the modified Bessel functions as described above, $\mu_t = \mu(h,\bar{\omega})$, $\mu_b = \mu(0,\bar{\omega})$, $\bar{\omega}_t = i2\bar{\omega}\sqrt{\mu_t} / |m|$ and $\bar{\omega}_b = i2\bar{\omega}\sqrt{\mu_b} / |m|$. The transfer function for the homogeneous case may be found by setting $m = 0$ in Equations (7) and (9) and solving the resulting boundary value problem, yielding

$$\frac{\tilde{\theta}_t}{\tilde{\theta}_b} = \frac{1}{\cos(\bar{\omega}^*) - \bar{I}\,\bar{\omega}^*\sin(\bar{\omega}^*)}, \tag{15}$$

where

$$\bar{\omega}^* = \frac{\bar{\omega}}{\sqrt{1 + i2\xi(\omega)}}. \tag{16}$$

Note that the foregoing transfer functions (14) and (15) for the proposed measurement approach correspond to the free-free or "spring base model" (Hardin, 1965), and are independent of the bottom platen's polar mass moment of inertia. Additionally, they are free of device-dependent torque-current calibration factors or a "system resonant frequency" as the first peak (ASTM D 4015; Hardin, 1965). If transducers are used to measure the motion of the top and bottom platens, the corresponding experimental transfer functions will also be free from extraneous damping effects from back-emf when drive-circuit voltages are used as a means to calculate the applied torque. Hardin (1965) also pointed out that due to the independence of the resonance ratio (the transfer function above) on the value of the forcing function and the base platen inertia, that the "best procedure studying soil properties would be to measure the resonance ratio."

Examples of the transfer functions derived above are shown in Fig. 1 for a homogeneous sample (m = 0) and a range of hysteretic damping ratios. Displaying transfer functions on a linear scale as shown in part (a) has been found useful in least-squares optimization procedures of the back-calculation of

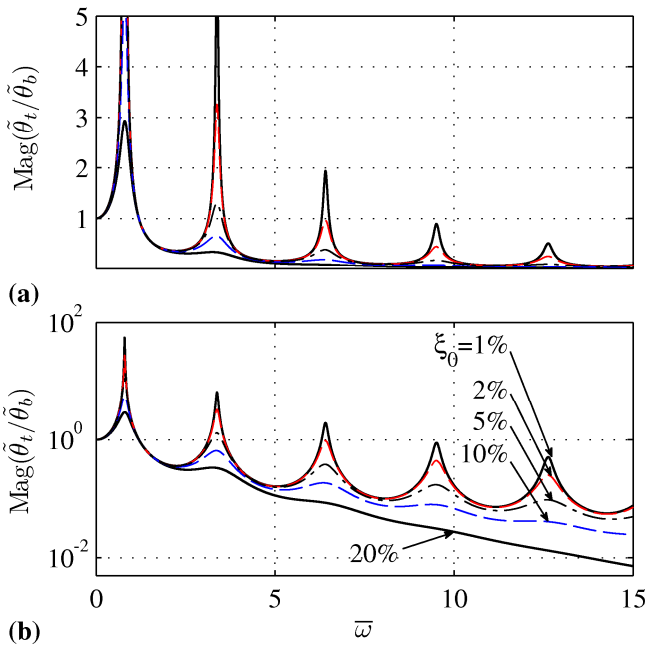

Fig. 1. Magnitude of transfer function for homogeneous (m = 0) free-free resonant column sample with hysteretic damping. (a) linear scale typically used in least-squares modulus/damping optimization procedure, (b) logarithmic scale for examining damping characteristics at high frequencies.

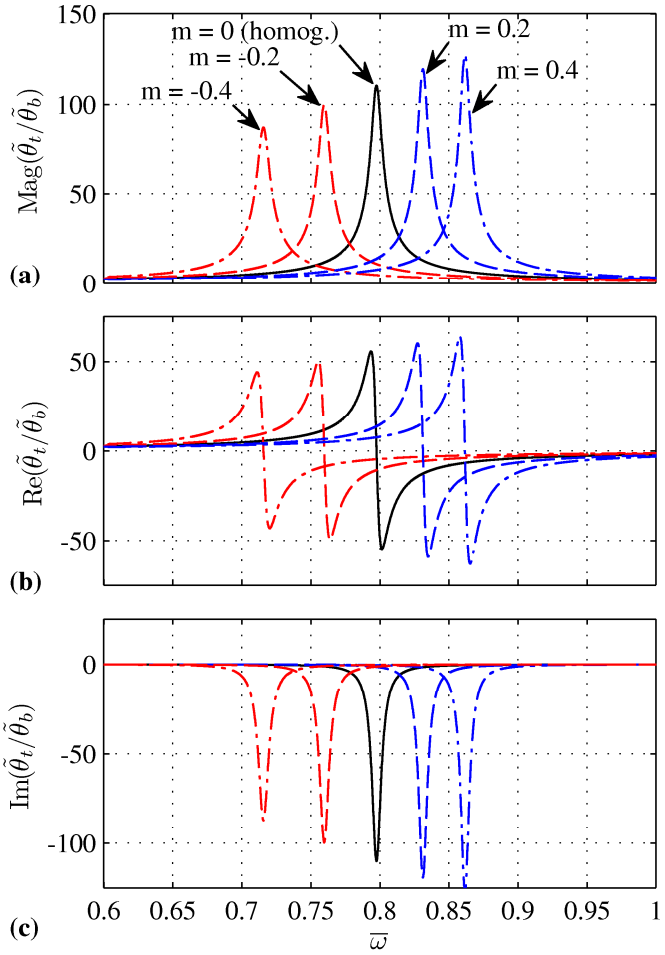

Fig. 2. Effect of linear shear modulus heterogeneity of Equation (3) on first peak of free-free resonant column transfer function. (a) magnitude, (b) real component, (c) imaginary component. Hysteretic damping, $\xi_0 = 0.5\%$.

modulus and damping values. To observe the effect of damping on the higher modes in more detail, a semi-log plot of the transfer function is also useful (see Fig. 1b). To facilitate their comparison to the experimentally measured resonant column transfer functions, all theoretical curves in this paper will be presented for the sample dimensions and properties given above, with a top-platen inertia ratio of $\bar{I}$ = 1.224.

The effects of a linear height-wise variation in the shear modulus on the first peak of the transfer function are illustrated via comparison of Equations (14) and (15) in Fig. 2 for a hysteretic damping ratio $\xi(\omega) = \xi_0 = 0.5\%$. The magnitude of the transfer function, as shown in Fig. 2a, is commonly used to convey information about resonant frequencies and damping behavior. In this study, the real and imaginary components shown in Fig. 2b and Fig. 2c are preferred over magnitude and phase for use in least-squares-type error optimization algorithms to calibrate dynamic material properties, as the real and imaginary components share common units. As shown in Fig. 2, both the frequency and amplitude of the fundamental peak increase for positive values of *m* (modulus increasing towards the sample top), and decrease for negative values of *m*. Traditional resonant column testing techniques involve the application of sinusoidal loading at a number of excitation frequencies in order to measure the fundamental peaks of the type shown in Fig. 2. Random vibration techniques, on the other hand, permit measurement of the system response at many closely spaced frequencies over a wide bandwidth in a matter of a few seconds, allowing one to efficiently measure not only the fundamental peak, but also those of higher modes with suitable instrumentation. The increased amount of information afforded by measuring the system response over a greater bandwidth than just the neighborhood of the fundamental peak naturally provides the possibility of a more detailed validation and calibration of numerical models, as well as the study of frequency dependence of modulus and damping characteristics. For example, the transfer function of Fig. 2 is shown for an enlarged frequency range $0 \le \bar{\omega} \le 15$ in Fig. 3, illustrating the characteristics of the first five resonant peaks in relation to the heterogeneity parameter *m*. As shown in this figure, *m* can affect greatly the distribution of the modal resonant frequencies whose measurements can be achieved by the proposed test method.

While the analysis presented above enables a comparison of response functions for shear modulus profiles which share a common value G_0 at the bottom of the sample, further insight can be gained by having modulus profiles that share a

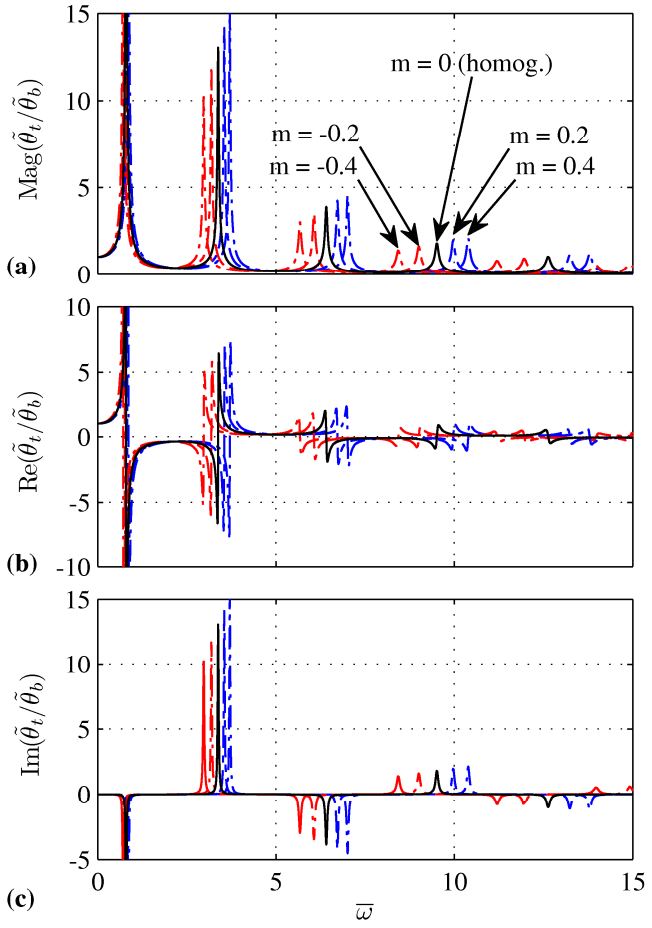

Fig. 3. Effect of linear shear modulus heterogeneity of Equation (3) on first 5 peaks of free-free resonant column transfer function. (a) magnitude, (b) real component, (c) imaginary component. Hysteretic damping, $\xi_0 = 0.5\%$.

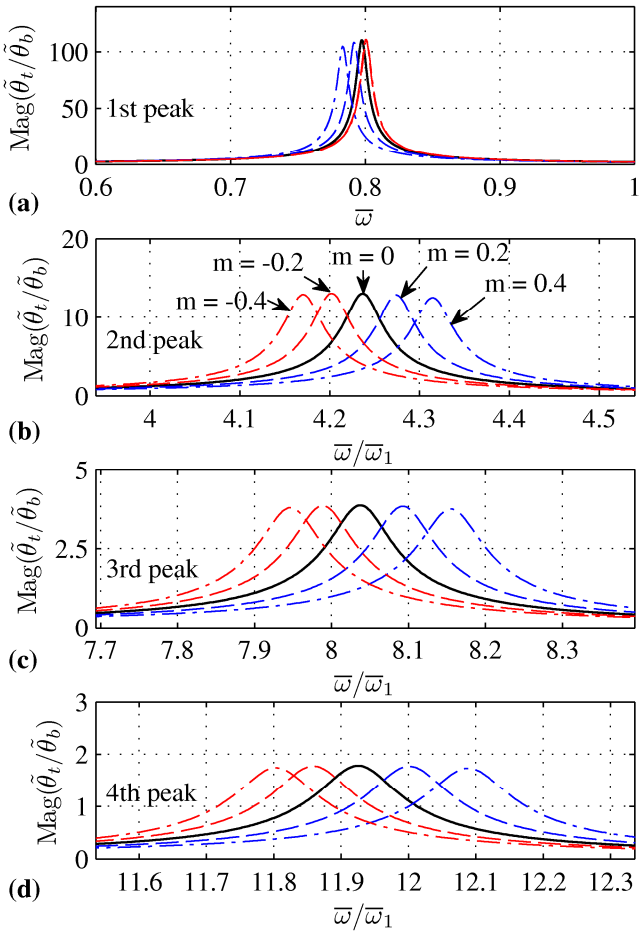

Fig. 4. Effect of linear shear modulus heterogeneity of Equation (17) on first 4 peaks of free-free resonant column transfer function. (a) first peak frequency $\bar{\omega}_1$, (b) 2nd (c) 3rd (d) 4th peak frequency ratios $\bar{\omega}_n/\bar{\omega}_1$.

common value at mid-height. Although this could be achieved by scaling G_0 in Equation (3) and adjusting Equation (8) to achieve a common frequency normalization, a direct formulation is equally convenient. For this purpose, the shear modulus profile may be taken as

$$G(z) = G_0\left(1 + m\left(\frac{z}{h} - \frac{1}{2}\right)\right), \qquad m \geq -2 \tag{17}$$

for which the average modulus has the value G_0 for all m. Proceeding as above, the term (mz/h) will be replaced with $m\left(z/h - 1/2\right)$ in Equations (7) and (9). It can be shown that the solution to the resulting differential equation will be the same as Equation (10) and the transfer function can again be represented by Equation (14), provided one sets

$$\mu(z,\bar{\omega}) = 1 + m\left(\frac{z}{h} - \frac{1}{2}\right) + i2\xi(\bar{\omega}). \tag{18}$$

As shown in Fig. 4a, the effect of the heterogeneity parameter m in Equation (17) on the amplitude and shape of the first peak of the transfer function is relatively minor for the range considered. The fundamental frequency $\bar{\omega}_1$ decreases for positive m and does not exhibit a systematic shift in relation to the value of m. Both of these characteristics are in contrast to the behavior for the modulus profile of Equation (3) (see Fig. 1). Similarly, the higher-order peaks can also be shown to exhibit non-systematic variations with changing m. However, a systematic trend is revealed by examining the frequency ratios $\bar{\omega}_n / \bar{\omega}_1$, $(n = 2,3,...)$, obtained by normalization of each curve's $\bar{\omega}$ by its fundamental peak frequency $\bar{\omega}_1$ (see Fig. 4b, c and d for the 2nd through 4th peaks). Such higher-order peak frequency ratios can be useful measures for the evaluation or calibration of stiffness and damping properties of various theoretical models against those of measured data. For example, Fig. 5 and Fig. 6 show the theoretical transfer functions for the shear modulus profiles of Equation (17), calibrated to the fundamental peak frequency $f_1 = 102$ *Hz* of the soil column at a confining pressure of 10 psi (68.9 kPa).

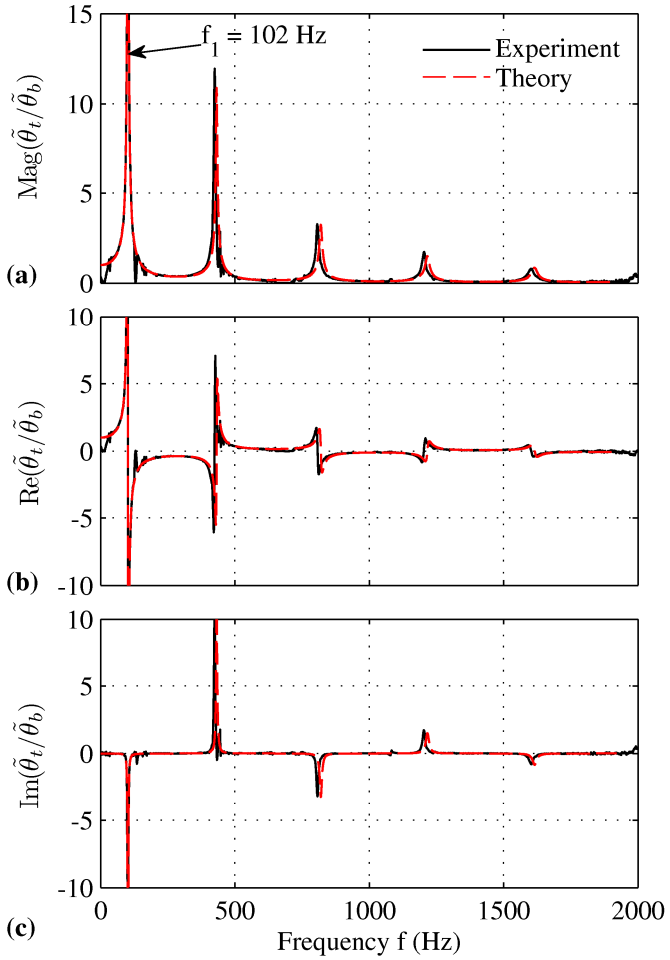

Fig. 5. Theoretical transfer function for homogeneous sample fit to first peak of measured response at f_1 = 102 Hz. Calibrated homogeneous shear modulus G= 109.5MPa, hysteretic damping ratio ξ_0 = 0.6%. Specimen confining pressure 10 psi (68.9 kPa).

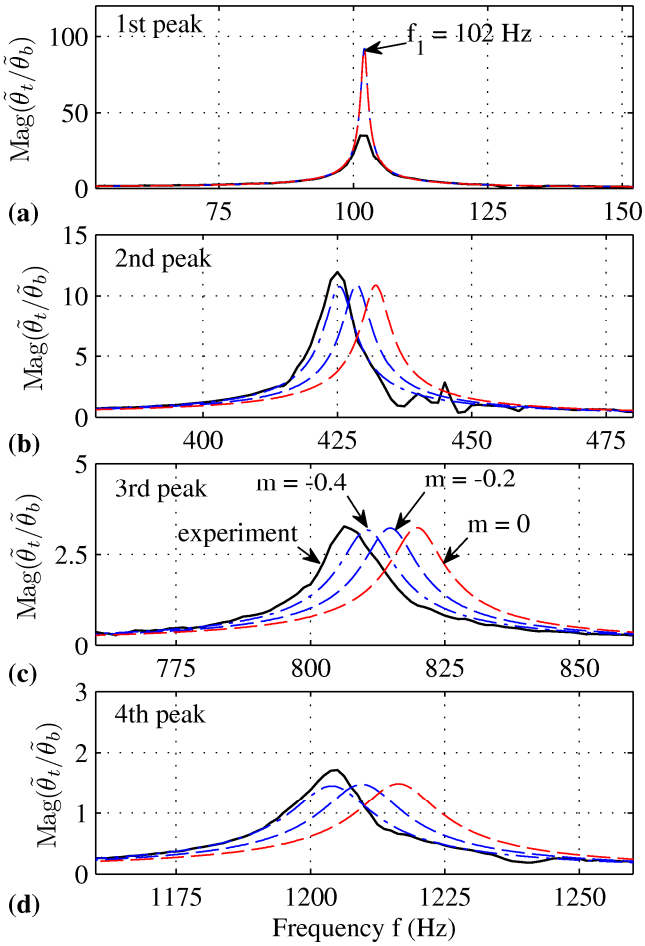

Fig. 6. Theoretical transfer function for vertically heterogeneous sample with shear modulus $G(z) = G_0(1 + m\,(z/h - 1/2))$, hysteretic damping ratio $\xi_0 = 0.6\%$. Specimen confining pressure 10 psi (68.9 kPa). (a) first peak calibrated to measured f_1 = 102 Hz, (b), (c), and (d) frequencies of 2nd – 4th peaks. Calibrated $G_0(MPa)$ =109.5, 108.6 and 108.5 for m=0, -0.2 and -0.4.

The theoretical resonant frequencies of the higher modes appear to be in very good agreement with the measured values when plotted over the full measurement bandwidth of 2 kHz as can be seen in Fig. 5. Closer examination of the 2nd through 4th peaks as shown in Fig. 6 reveals that the homogeneous-modulus solution predicts peak frequencies that are approximately 1-2% higher than measured. Based on the results shown in Fig. 4, one possible explanation for the measured peak frequencies being slightly lower than those of the homogeneous case is a modulus increases with depth, which is not uncommon due to gravity and self-weight effects. To examine the possible effects of a linear height-wise shear modulus variation on the higher-mode's resonant frequencies, transfer functions for the modulus profile of Equation (17) with m = –0.2 and –0.4 are also included in Fig. 6. Although a good match of the higher-order peaks is obtained with m = –0.4, calculations based on the relations of Hardin and Drnevich (1972) indicate that such a variation in shear modulus (i.e. –/+20% of G_0 at the sample top and bottom) is perhaps too large to be the sole explanation for the discrepancy. Other physical conditions of the test such as imperfect platen contacts and higher-order heterogeneity can also contribute to the cause and might warrant further investigation.

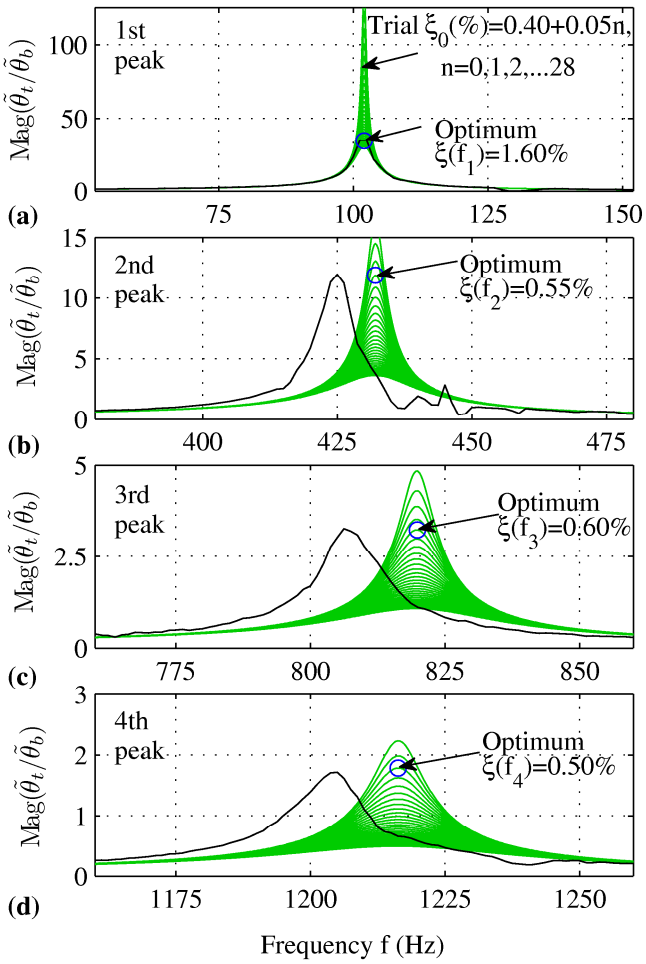

Fig. 7. Determination of optimum damping ratios to match first 4 measured peak amplitudes. Transfer function for homogeneous sample fit to first measured peak f_1 = 102 Hz. Calibrated shear modulus G= 109.5MPa. Specimen confining pressure 10 psi (68.9 kPa).

INVESTIGATION OF FREQUENCY-DEPENDENT DAMPING BEHAVIOR

Owing to the data it can generate for multiple resonant regimes efficiently, the random-vibration resonant column method can be naturally used to study the frequency dependence of the soil's damping properties. As noted by Hardin (1965), the amplitudes of the theoretical transfer function peaks in Fig. 6 are related to the damping ratio and may therefore be used to determine an experimental damping ratio in the neighborhood of a given peak. With the frequency-independent hysteretic damping ratio $\xi_0 = 0.6\%$ in Fig. 5 and Fig. 6 , the three measured higher-order peaks are matched reasonably well by the theory, but a larger damping ratio is required near the frequency of the fundamental peak. Flexible in allowing frequency-dependent material properties, the proposed formulations permit a variety of forms for the generalized damping ratio $\xi(\omega)$. To investigate the frequency-dependence of the soil's damping behavior,

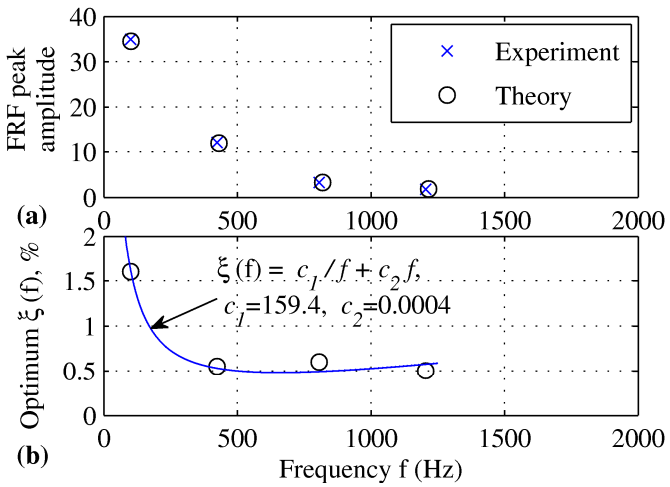

Fig. 8. Least squares approximation of first four optimum damping ratios by the function $\xi(f) = c_1 / f + c_2 f$ to match measured FRF amplitudes. (a) transfer function (FRF) amplitudes and frequencies, (b) optimum damping ratios.

theoretical transfer functions for a range of hysteretic damping ratios may be calculated and the best-fit damping ratio at the frequency of each peak identified as that which provides the closest match of the measured peak amplitude. An example of this procedure is illustrated in Fig. 7, from which the optimum damping ratios for the fundamental and higher-order peaks are identified as $\xi(f_1) \approx 1.6\%$, $\xi(f_2) \approx 0.55\%$, $\xi(f_3) \approx 0.60\%$, and $\xi(f_4) \approx 0.50\%$. The amplitudes of these measured and theoretical transfer function peaks are displayed on a common scale in Fig. 8a and the corresponding damping ratios are shown in Fig. 8b. To investigate the behavior of the theoretical transfer function for a frequency-dependent damping ratio, the values shown in Fig. 8b are fit in a least-squares sense by the function

$$\xi(f) = \frac{c_1}{f} + c_2 f \qquad (19)$$

as shown in Fig. 8b. Using this formula for damping in Equation (18) results in a transfer function that matches the peak frequencies and magnitudes reasonably well, as shown in Fig. 9.

CONCLUSIONS

In this study, the experimental setup and analytical formulation for a free-free resonant column device are outlined in the application of the random-vibration method. The free-free boundary conditions enable the direct measurement of tangential accelerations at the sample's top and bottom boundaries, permitting the determination of experimental transfer functions on the basis of only end-platen accelerations. This avoids the need of device-dependent torque-current calibration factors commonly required when

using fixed-free RC devices. Because the experimental free-free transfer function measurement approach presented herein also does not involve the use of excitation voltages or currents from the coil drive-circuit, the technique also does not suffer from errors in damping measurements that can be caused by effects of back-emf. Since the motion of the bottom platen is measured, knowledge of its polar mass moment of inertia is not necessary for the calculation of the transfer functions, even though it is a factor in the mode shape profiles and shear strain variations (Hardin, 1965). As one more practical advantage, the experimental and analytical transfer functions do not contain a device-dependent "system resonant frequency" (see, e.g. ASTM D 4015) which must typically be determined when using free-free RC devices.

To investigate the effects of a height-wise variation of shear modulus and the frequency-dependence of damping, theoretical transfer functions were presented for a linear variation in shear modulus with depth and a generalized frequency dependent damping ratio. The ability to explore and characterize the material parameters of soil for general modal synthesis involving multiple resonant regimes is apt to be of fundamental relevance to understanding the intricacy and common approximations in site response analysis in soil dynamics and earthquake engineering.

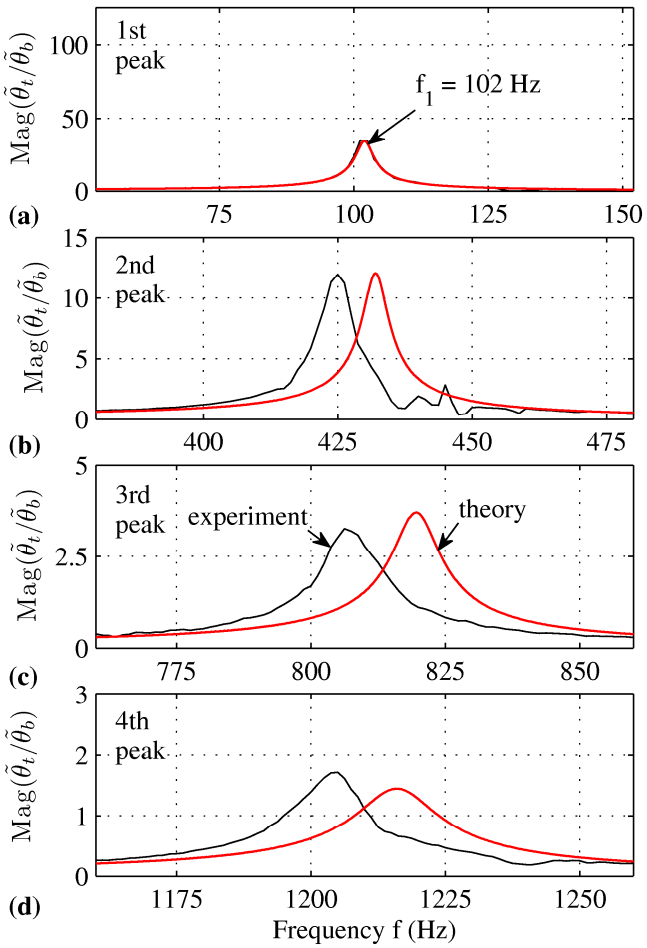

Fig. 9. Improved fit of measured peak amplitudes using frequency dependent damping ratio. Homogeneous shear modulus G= 109.5MPa, $\xi(f) = 159.4/f + 0.0004 f$. Specimen confining pressure 10 psi (68.9 kPa).

REFERENCES

Aggour, M. S., Taha, M. R., Tawfiq, K. S., and Amini, F. [1989]. "Cohesive soil behavior under random excitation conditions", Geotech. Testing J., 12(2), pp. 135-142.

Aggour, M. S., Tawfiq, K. S., and Taha, M. R. [1988]. "Impulse and random testing of soils", Earthquake Eng. and Soil Dyn. II - Recent Advances in Ground-Motion Evaluation, GSP, pp. 346-358.

Al-Sanad, H., Aggour, M., and Yang, J. [1983]. "Dynamic Shear Modulus and Damping Ratio from Random Loading Tests", GTJ, 6(3), pp. 120-127.

Amini, F., Tawfiq, K. S., and Aggour, M. S. [1988]. "Cohesionless Soil Behavior Under Random Excitation Conditions", J.Geotech. Engrg., 114(8), pp. 896-914.

Ashlock, J. C. and Pak, R. Y. S [2010, in press], "Applications of Random Vibration Techniques to Resonant Column Testing", Proc. GeoFlorida 2010, ASCE.

Bendat, J. S., and Piersol, A. G. [1986]. "*Random data: analysis and measurement procedures*", New York : Wiley, New York.

Cascante, G., and Santamarina, C. [1997]. "Low Strain Measurements Using Random Noise Excitation", GTJ, 20(1), pp. 29-39.

Cascante, G., Santamarina, C., and Yassir, N. [1998]. "Flexural excitation in a standard torsional-resonant column device", Canadian Geotech. J., 35(3), pp. 478-490.

Cascante, G., Vanderkooy, J., and Chung, W. [2003]. "Difference between current and voltage measurements in resonant-column testing", Canadian Geotech. J., 40(4), pp. 806-820.

Cascante, G., Vanderkooy, J., and Chung, W. [2005]. "A new mathematical model for resonant-column measurements including eddy-current effects", Canadian Geotech. J., 42(1), pp. 121-135.

Drnevich, V. P. [1978], "Resonant Column Testing – Problems and Solutions", Dynamic Geotech. Testing, ASTM STP 654, pp. 384-398.

Drnevich, V. P., Hardin, B. O., and Shippy, D. J. [1978]. "Modulus and Damping of Soils by the Resonant-Column Method", ASTM Spec. Tech. Pub., pp. 91-125.

Fratta, D., and Santamarina, J. C. [1996]. “Wave propagation in soils: Multi-mode, wide band testing in a waveguide device”, Geotech. Testing J., 19(2), pp. 130-140.

Hardin, B. O. [1965]. “The nature of damping in sands”, ASCE J Soil Mech. found. Div., SM 1, pp. 63-97.

Hardin, B. O. & Drnevich, V. P. [1972]. “Shear modulus and damping in soils: design equations and curves.” J. Soil Mech. Found. Div. Proc. ASCE 98, No. SM7, pp. 667–692.

Hardin, B. O. & Richart, F. E. [1963]. “Elastic wave velocities in granular soils”, J. Soil Mech. Found. Div. Proc. ASCE 89, No. SM1, pp. 33–65.

Iwasaki, T., Tatsuoka, F. & Takagi, Y. [1978]. “Shear moduli of sands under cyclic torsional shear loading”, Soils Found. 18, No. 1, pp. 39–56.

Khan, Z. H., Cascante, G., and El-Naggar, M. [2008]. “Evaluation of the first mode of vibration and base fixidity in resonant-column testing”, Geotech Testing J., 31(1), pp. 65-75.

Khan, Z. H., Cascante, G., El Naggar, M. H., and Lai, C. G. [2008]. “Measurement of frequency-dependent dynamic properties of soils using the resonant-column device”, J. Geotech. Geoenviron. Engrg., 134(9), pp. 1319-1326.

Li, X. S., Yang, W. L., Shen, C. K., and Wang, W. C. [1998]. “Energy-injecting virtual mass resonant column system”, J. Geotech. Geoenviron. Engrg., 124(5), pp. 428-438.

Pak, R. Y. S., Ashlock, J. C., Kurahashi, S., and Abedzadeh, F. [2008]. “Parametric Gmax sounding of granular soils by vibration methods”, Geotechnique, 58(7), pp. 571-580.

Rix, G. J. and Meng, J. [2003]. “A non-resonance method for dynamic soil properties”, in De Benedetto et al. (eds), Deformation Characteristics of Geomaterials, pp. 57-62.

Wang, Y., Cascante, G., and Santamarina, J. C. [2003]. “Resonant column testing: The inherent counter EMF effect”, Geotech. Testing. J., 26(3), pp. 342-352.

Yong, R. N., Akiyoshi, T., and Japp, R. D. [1977]. “Dynamic Shear Modulus of Soil Using a Random Vibration Method”, Soils and Found., 17(1), pp. 1-12.